Application of the **NOTCH STRESS INTENSITY** and **CRACK PROPAGATION APPROACHES** to weld toe and root fatigue

C. Fischer, O. Feltz, W. Fricke and P. Lazzarin

ABSTRACT

Several fatigue failures are initiating from the root of non-penetrating welds, which are widely applied in several industrial sectors. The structural optimization and reduction of weld material increase the danger of root cracking. The fatigue assessment during design is mainly based on the nominal, structural hot-spot or notch stress approach. These approaches are only partly applicable to weld roots, give rough estimates such as the nominal stress approach or over-conservative life estimation such as occasionally the notch stress approach when keyhole notches are modelled. An alternative assessment is possible with the crack propagation approach assuming the non-welded root gap and a short crack at the weld toe as initial cracks. A new approach is the notch stress intensity approach (N-SIF approach) which is able to assess the fatigue life of V-shaped notches at weld toes as well as crack-like notches at weld roots using the strain energy density around the notch. Both approaches are applied to different joints where toe and root failures are probable. The results are compared with a previous analysis using the notch stress approach. Fatigue test results are also available for a comparison which allows to draw conclusions with respect to the approaches for an appropriate fatigue strength assessment.

IIW-Thesaurus keywords: Crack propagation; Failure; Fatigue strength; Notch effect; Weld toes; Welded joints.

Nomenclature

a	weld throat thickness
a_i	initial crack length
a_c	critical crack length
C	material constant
da/dN	crack propagation rate
E	modulus of elasticity
E'	modified modulus of elasticity
e_1, e_2	parameters for dependency from α
K_c	critical stress intensity factor
K_1, K_2	stress intensity factor for Mode I and Mode II loading
ℓ	length
λ_1, λ_2	eigenvalues of the stress field for K_1 and K_2 modes
m	slope exponent of S-N curve
m	material constant (in Paris equation)
N	number of load cycles
P_s	probability of survival
R	stress ratio (lower stress / upper stress)
R_{eH}	yield stress
R_0	control radius
R^*	enlarged control radius
r_{ref}	reference radius ref. to notch stress
t	plate thickness
T_σ	scatter index ref. to fatigue strength for $P_s = 10$ and 90 %
W	elastic strain energy density

Greek symbols

α	half opening angle of V-notch
Δa	crack increment
ΔK	range of stress intensity factor
ΔK_{th}	threshold range of stress intensity factor
$\Delta\sigma_c$	characteristic fatigue strength
$\Delta\sigma_{eq}$	equivalent stress range
$\Delta\sigma_n$	nominal stress range
$\Delta\sigma_T$	range of T-stress (parallel to slit)
ΔW	range of elastic strain energy density
ΔW_T	range of elastic strain energy density due to T-stress
ν	Poisson's number
σ	stress

1 Introduction

Fatigue is one of the major design criteria in cyclic stressed welded structures. Different approaches exist for the fatigue assessment. Apart from the nominal stress approach, the so-called structural hot-spot stress approach is widely used in fatigue design. It has the advantage that the stress increase due to the structural configuration, which varies to a large extent, can be rationally considered [1]. One disadvantage of the approach is that the structural hot-spot stress cannot consider the intensified local stress at the toe of load carrying fillet welds in comparison to non-load carrying fillet welds. Therefore, two different fatigue classes have been introduced in the Fatigue Design Recommendations of the International Institute of Welding [2], i.e. FAT 90 for load carrying and FAT 100 for non-load carrying fillet welds.

Doc. IIW-2206, recommended for publication by Commission XIII "Fatigue of Welded Components and Structures" and by Commission XV "Design, Analysis and Fabrication of Welded Structures."

Alternative approaches have been developed to consider this effect in the structural stress, which are summarized in [3]. However, most of the structural stress approaches are restricted to the assessment of weld toe failures. Therefore, refined approaches are to be applied if also weld root failures have to be assessed and compared with each other. One of these is the effective notch stress approach [2, 4], using the elastic stress in the weld toe or root rounded by $r_{ref} = 1$ mm as fatigue parameter in plates with thickness $t \geq 5$ mm. The corresponding fatigue class is FAT 225. A disadvantage of this approach might be that usually a 'keyhole' notch is arranged at weld roots producing an additional notch effect particularly at the end of the non-fused root faces of non-penetrating fillet welds when loaded parallel to the slit.

An alternative is the recently developed notch stress intensity factor (N-SIF) approach, using the N-SIF of V-shaped notches as fatigue parameter [5, 6]. Typically weld toes with a notch opening angle of 135° and slit ends at weld roots with an opening angle of zero degrees are considered. An extremely fine FE mesh can be avoided by utilizing the strain energy density close to the notch, which can be converted into the N-SIF or directly used as fatigue parameter [7].

Contrary to the approaches mentioned, the crack propagation approach considers the crack growth using the well-known relation between crack growth rate and stress intensity factor range by Paris and Erdogan [8]. The crack propagation approach has been applied to the fatigue assessment of weld toes and roots for a long time, usually neglecting the crack initiation phase by assuming an initial crack length in the order of 0.1 mm (so-called equivalent initial flaw-size concept). At weld roots, the whole slit length is assumed as initial crack.

The 'classical' case for the fatigue assessment of weld toes and roots is the cruciform joint with load-carrying fillet welds, where the non-welded root faces are oriented perpendicular to the load direction (Figure 1). Maddox [9] applied the crack propagation approach to this case, deriving ranges of geometry parameters where toe or root failure dominates. Petershagen [10] obtained similar results by applying the effective notch stress approach.

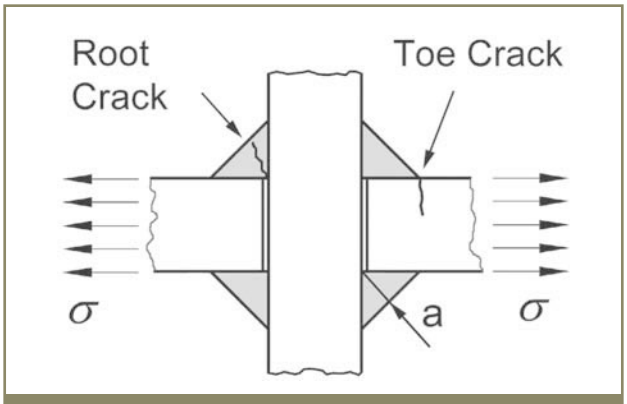

Figure 1 – Weld toe and root crack in a cruciform joint

More complex is the case where the load is acting parallel to the slit (i.e. vertical in Figure 1). If only transverse stiffeners are attached, fatigue cracks usually initiate at the weld toes. If, however, cover plates are attached and the loaded main plate is interrupted, weld root failures might occur, particularly if the weld throat thickness is rather low.

Such cases have been investigated by Fricke and Feltz [11], applying the nominal, different structural and the effective notch stress approaches and comparing the fatigue lives with test results obtained from specimens in as-welded state. The results were not satisfactory with respect to the identification of the fatigue-critical location and the predicted fatigue lives.

In this paper, the notch stress intensity approach and the crack propagation approach are applied to these cases with the objective to correctly predict the critical location. As the fatigue tests have meanwhile been supplemented by stress-relieved specimens, the specimens and total results are briefly described at first, before the approaches for fatigue strength assessment are applied.

2 Fatigue tests

2.1 Test specimens

Two different types of specimens were tested, see Figure 2, the *lap joint* with an interrupted main plate and *cover plates* on a continuous main plate. In the first case, the fillet welds are full-load carrying, while those at cover plates are partial-load carrying, which has an effect on the local stresses at the weld toe and root. Figure 2 shows the geometry of the specimens. A plate thickness of 12 mm and two different weld throat thicknesses of $a = 3$ and 7 mm were chosen resulting in four different types of specimens, denoted L.3, L.7, C.3 and C.7.

The test specimens were fabricated from structural steel S355 having a nominal yield limit $R_{eH} = 355$ N/mm². In total, 10 specimens were fabricated for each geometry, i.e.

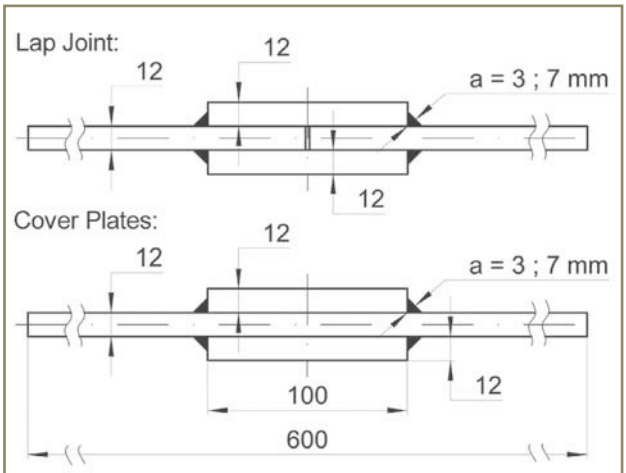

Figure 2 – Geometry of the specimens for the fatigue tests

for each of the four test series in as-welded state and the same number in the stress-relieved state. Further details of the specimens and the tests in as-welded state are given in [11].

2.2 Fatigue tests and results

The fatigue tests were performed with constant load amplitudes in a resonance pulsator at a frequency of approximately 30 Hz and room temperature. The fatigue tests were performed at different load levels, corresponding to nominal stress ranges in the plate in front of the weld between $\Delta\sigma_n = 90$ and 210 MPa. The stress ratio was $R \approx 0$.

Depending on the type of specimen, fatigue crack initiation was observed either at one of the weld toes, running through the main plate, or at one of the weld roots, propagating through the weld throat. Fracture of the specimen was taken as failure criterion as usual for small-scale specimens. Mainly weld toe failures occurred, while weld root cracks were observed only in part of the specimens with a weld throat thickness $a = 3$ mm, mostly in the lap joints carrying more stress. Table 1 gives an overview of the crack locations.

The fatigue lives of each test series were statistically evaluated assuming forced slope exponent $m = 3$ for the S-N curves being typical for welded joints.

Table 1 – Number of failures sorted by location

	- as-welded -		- stress-relieved -	
	toe	root	toe	root
L.3	-	10	-	10
C.3	7	3	10	-
L.7	10	-	10	
C.7	10	-	10	

Figure 3 shows the fatigue lives of all specimens with weld toe failures. All results seem to fall into one scatter band although the stress-relieved specimens (full symbols) show a lower fatigue strength. It is interesting to note that no difference is recognizable between lap joints (full-load carrying) and cover plates (partial-load carrying). The evaluated characteristic fatigue strength for $N = 2 \times 10^6$ and a survival probability $P_s = 97.7$ % is $\Delta\sigma_c = 73$ MPa (78 MPa if only as-welded specimens are evaluated). The corresponding scatter index T_σ related to probabilities of survival $P_s = 10$ and 90 % is 1.46.

The fatigue lives of the lap joints with throat thickness $a = 3$ mm showing root failures are summarized in Figure 4. It should be noted that the nominal stress is based on the main plate. Although the stress-relieved specimens seem to have slightly larger fatigue strength, the results were statistically evaluated together yielding a characteristic fatigue strength $\Delta\sigma_c = 47$ MPa (41 MPa for as-welded specimens only). It should be noted that the S-N curve seems to have a shallower slope causing a wide scatter band when $m = 3$ is assumed.

3 Fatigue assessment with the notch stress intensity approach

3.1 Overview of the approach

The theoretically infinite stress at sharp V-notches with notch opening angle 2α can be described by a notch stress intensity factor (N-SIF) in a similar way as for crack tips. Local stress distributions in plane configurations are given as a combination of a symmetric and skew-symmetric stress field. The N-SIFs K_1 and K_2 for Mode I

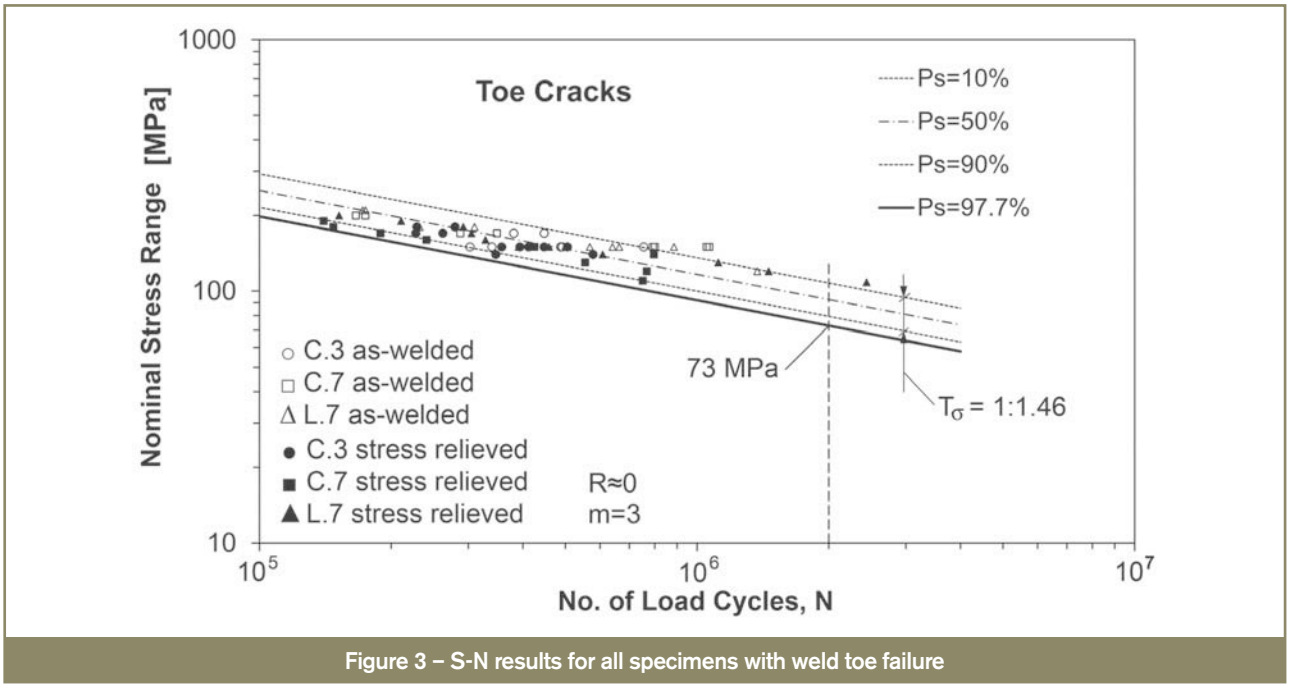

Figure 3 – S-N results for all specimens with weld toe failure

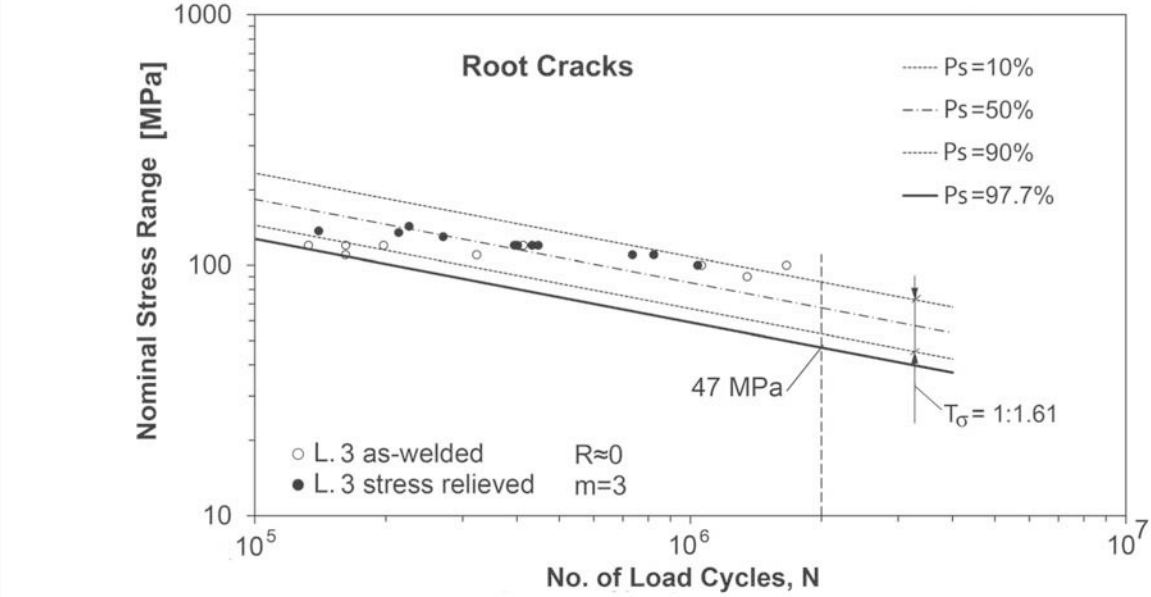

Figure 4 – S-N results for all L.3-specimens with weld root failure

and II loading quantify the magnitude of the asymptotic stress distribution according to the exact solution of Williams [12].

The N-SIFs can directly be used to describe the crack initiation at sharp corners [13]. Tovo and Lazzarin [5] developed an N-SIF approach for welded joints and showed that fatigue test results of various welded joints form an S-N curve with reasonable scatter if based on N-SIF.

The N-SIF approach requires knowledge of the elastic stress field in the region very close to the notch tip. Similar as for the stress analysis at crack tips, finite element meshes must be very fine in this region. However, the N-SIFs K_1 and K_2 can be related to the total elastic strain energy W averaged over a cylindrical sector with the characteristic radius R_0 in the case of the Mode I and Mode II stress distributions under plane strain conditions by the following equation:

$$W = \frac{e_1}{E}\left[\frac{K_1}{R_0^{1-\lambda_1}}\right]^2 + \frac{e_2}{E}\left[\frac{K_2}{R_0^{1-\lambda_2}}\right]^2 \qquad (1)$$

where

E = Young's modulus

λ_1, λ_2 = the eigenvalues of the stress field for K_1 and K_2 modes (see Figure 5)

e_1, e_2 = parameters depending on the notch opening angle 2α.

When 2α is 135°, a typical value for fillet-welded joints, the Mode I stress distribution is singular ($1 - \lambda_1 = 0.326$), whereas the Mode II distribution is not ($1 - \lambda_2 = -0.302$). Consequently, Equation (1) may be reduced to the first term. The parameter e_1 is 0.1172 for this opening angle and for Poisson's ratio $\nu = 0.3$, given in [14].

The control radius R_0 is material-dependent and has been proposed in [6, 14] to be 0.28 mm considering the failure behaviour of conventional fillet-welded joints at steel under Mode I loading. For an opening angle of 0°, this value is conservative because corresponding considerations would result in $R_0 = 0.36$ mm.

The correlation between the averaged elastic strain energy (SED) and the N-SIF offer a practical way of computing the relevant fatigue parameter with a coarser finite element model. The averaged SED can directly be used as fatigue parameter, allowing to include the results of different notch opening angles (i.e. weld toes and roots) within the same diagram (whereas the N-SIFs have different units). An evaluation for 650 welded joints has been given in [7], see Figure 6.

A uniform control radius $R_0 = 0.28$ mm has been used for both weld toe and weld root failure. The thickness of the

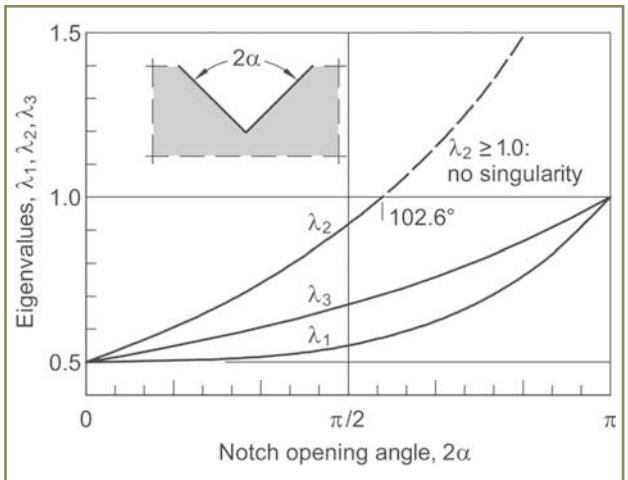

Figure 5 – Eigenvalues defining the order of stress singularity at sharp V-notches depending on 2α from [4])

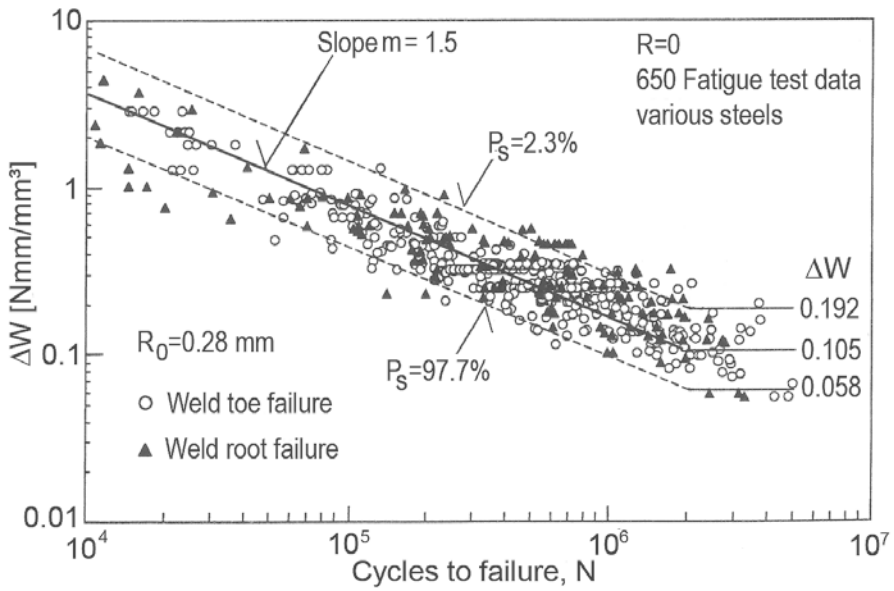

Figure 6 – Fatigue strength of fillet-welded joints as function of the range of the averaged strain energy density ΔW [7]

main plate ranged from 6 to 100 mm, so that its effect is included. The scatter band given in Figure 6 refers to ± two standard deviations, giving a characteristic fatigue strength of $\Delta W = 0.058$ Nmm/mm³.

A relationship with stresses can be found by the simple expression

$$\Delta\sigma_{eq} = \sqrt{2E \cdot \Delta W} \qquad (2)$$

with

$E' = E / (1-\nu^2)$ for plane strain conditions [7]. Equation (2) describes the equivalent stress for a calculated SED averaged over a volume. By this the vertical axis in Figure 6 could be converted into an equivalent stress range, resulting in a slope exponent $m = 3$ due to the square root in Equation (2).

3.2 Finite element analysis

The approach based on the averaged SED would require a finite element size of 0.28 mm or less in the notch area. Figure 7 shows very fine meshes with an element size at the weld toe and slit tip of approximately 0.03 mm. Also indicated is the area within the control radius $R_0 = 0.28$ mm, where the averaged elastic strain energy has to be determined.

If the stress field is close to the Mode I stress distribution, Equation (1) allows the conversion of ΔW from the radius R^* to R_0 (neglecting K_2):

$$\Delta W(R_0 = 0.28) = \Delta W(R^*) \cdot \left(\frac{R_0}{R^*}\right)^{2(\lambda_1 - 1)} \qquad (3)$$

Lazzarin *et al.* [7] have shown that the computation of the averaged SED for a control radius of $R^* = 1$ mm and converting it to 0.28 mm yields results with sufficient accuracy at the weld toe where only Mode I stress distribution is singular. In principle, Equation (3) can be used also under mixed mode conditions, when the degree of singularity of the Mode I and Mode II stress fields is the same, like it occurs at the weld root region ($\lambda_1 = \lambda_2 = 0.5$). However, at the roots of non-penetrating welds with loading parallel

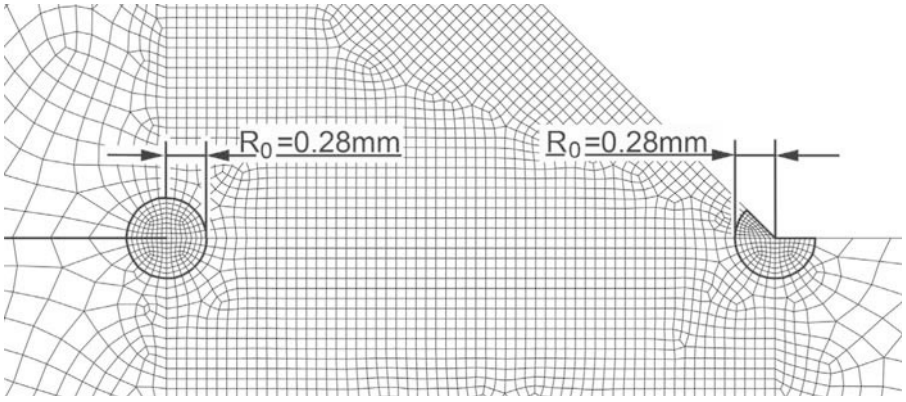

Figure 7 – Very fine mesh model of weld root and toe

to slit the effect of the T-stress (i.e. the constant stress component parallel to the slit [15]) has to be taken into account. This means that the contribution of the T-stress σ_T to the strain energy density at weld roots, i.e.

$$\Delta W_T = \sigma_T^{\,2} / 2E \qquad (4)$$

has to be deducted from the range of the averaged strain energy $\Delta W(R^*)$ before converting the SED by Equation (3). Doing so, it is possible to compute the increase to the local strain energy density due only to the singular stress fields. After conversion ΔW_T has to be included again.

Lazzarin *et al.* [7] proposed to use a mesh with triangular elements around the notch tip having a length of $\ell = 1$ mm so that only a relatively coarse mesh is needed. Only weld toe failures were explicitly considered in [7]. Figure 8 extends the procedure from the weld toe to the weld root and shows parts of corresponding 2D element models of the four types of specimens shown in Figure 2 which have been created in ANSYS, using plane strain elements with quadratic shape function.

Based on the experience gained with previous structural and notch stress investigations [11], contact between the main and the attached plate was considered by using contact elements without friction.

3.3 Results and comparison with the tests

The averaged SED has been determined for the control sector using a subroutine in ANSYS. In addition to the meshes in Figure 8, relatively coarse meshes with an element length $\ell = 0.28$ mm at the notch tip were created, avoiding the conversion of the SED from $R^* = 1$ mm to 0.28 mm. The computed range of the SED, ΔW, is given in Table 2 for a nominal stress range $\Delta\sigma_n = 150$ MPa being typical for the tests.

The difference between the coarse and fine meshes is small as long as the element length ℓ does not exceed 0.28 mm. For the coarse meshes with $\ell = 1$ mm, the deviations are larger, but tolerable at the weld root, where the effect of the T-stress has been considered as described above. The calculation remains approximate because the effect of higher order terms (see [15]) has not been considered here for the sake of simplicity.

The largest SED-value at the toe or root determines the expected crack initiation site. It can be seen in Table 2 that the derived crack initiation site corresponds to the tests for three of the four types of specimens. Only the lap joint with $a = 7$ mm (L.7) shows the highest SED at the weld root, however, fatigue cracks occurred at the weld toe in the as-welded and stress-relieved state. It should be mentioned that the SED at the weld root would be slightly smaller if the control radius would be $R_0 = 0.36$ mm instead of 0.28 mm. This would change the crack initiation site.

The averaged SED has been computed for each specimen separately because the contact creates a slight non-linearity with increasing load. The results for the as-welded specimens are shown in the S-N diagram in

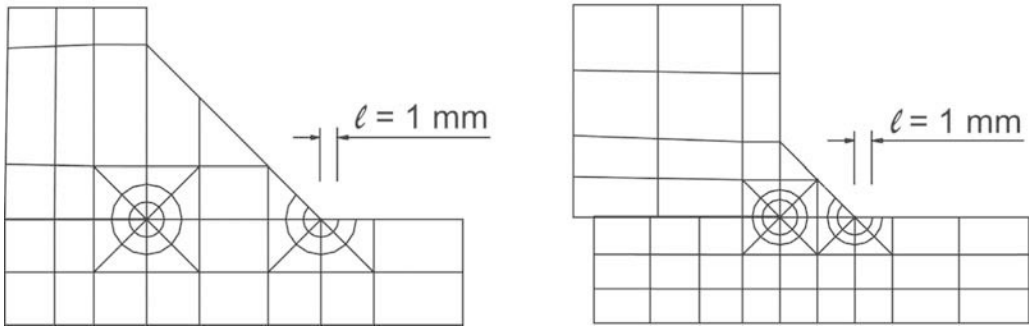

a) with $a = 7$ mm b) with $a = 3$ mm

Figure 8 – Coarse mesh models of the fillet welds

Table 2 – Computed ΔW from different meshes for $R_0 = 0.28$ mm and $\Delta\sigma_n = 150$ MPa

	ΔW [Nmm/mm³] for weld toe			ΔW [Nmm/mm³] for weld root[a)]			
	fine mesh (0.03 mm)	coarse mesh (0.28 mm)	coarse mesh (1 mm)	fine mesh (0.03 mm)	coarse mesh (0.28 mm)	coarse mesh (1 mm)	σ_T[b)] [MPa]
L.3	0.725	0.724 (0.2 %)	0.686 (5.4 %)	**1.107**	**1.089** (1.7 %)	**1.076** (2.8 %)	113
C.3	**0.352**	**0.352** (0.1 %)	**0.340** (3.4 %)	0.236	0.232 (1.6 %)	0.225 (4.5 %)	99
L.7	0.317	0.319 (0.7 %)	0.315 (0.4 %)	**0.393**	**0.395** (0.6 %)	**0.382** (2.9 %)	83
C.7	**0.241**	**0.244** (0.9 %)	**0.244** (1.1 %)	0.072	0.074 (2.3 %)	0.0678 (9 %)	83

a) Smaller values are obtained for $R_0 = 0.36$ mm.
b) Used for the conversion of ΔW from $R^* = 1$ mm to $R_0 = 0.28$ mm.
Deviations in % refer to fine mesh results. Expected failure location is indicated in bold.

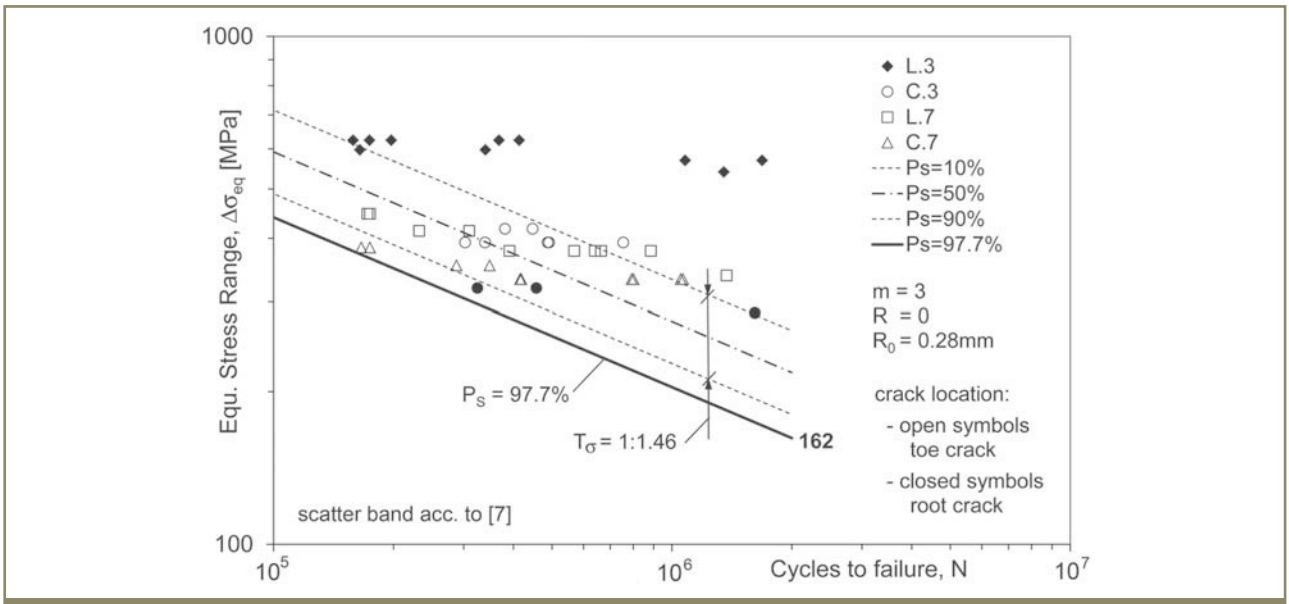

Figure 9 – S-N diagram showing the test results in terms of the equivalent stress

Figure 9, using the equivalent stress range according to Equation (2) on the vertical axis instead of the SED. Also included is the scatter band according to the evaluation in Figure 6, here in terms of the equivalent stress range.

Most of the results are within the scatter band except for the series L.3 failing from the weld root. The shallow slope of the S-N curve based on nominal stresses (Figure 6) can be recognized also here. The results are on the safe side – as in the nominal stress approach.

4 Fatigue assessment with the crack propagation approach

4.1 Overview of the approach

The crack propagation approach offers the computation of the number of cycles for a crack growing from an initial size a_i to a final (critical) size a_c on the basis of the power law according to [8]

$$\frac{da}{dN} = C(\Delta K)^m \qquad (5)$$

where

da/dN is the crack propagation rate,

ΔK is the range of the stress intensity factor (SIF) and

C and m are material constants.

Equation (5) describes the linear part of the crack growth in relation to ΔK in a double-logarithmic representation above the threshold value ΔK_{th} and below the critical SIF K_C where unstable fracture is expected. Additional effects such as the mean stress effect and crack closure can be considered e.g. by assuming an effective range of the SIF depending on the portion of the stress cycle where the crack is open.

Today, the crack propagation approach is mostly applied to the safety assessment of structures containing a defect or crack by computing its remaining life. However, the approach is also applied during design to cases where the crack initiation period is short. This is particularly the case for welded joints with incomplete penetration, where the crack may initiate from the weld root. For weld toes, a small initial crack depth between 0.05 and 0.25 mm is usually assumed to consider the effect of flaws (equivalent initial flaw-size concept).

BS 7608 [16] recommends for such an analysis to use material parameters $m = 3$ and $C = 3 \times 10^{-13}$ (units: N and mm), representing upper limit of the scatter band (97.7 % probability of survival). The IIW [2] recommends higher values for C.

4.2 Crack propagation analysis

The crack propagation analysis of the four types of specimens has been performed using the program FRANC2D [17] which applies the finite element method for the computation of the SIF. Using a relatively fine two-dimensional basic mesh [Figure 10 a)], the elements around the crack tip are deleted [Figure 10 b)] and the area is re-meshed with appropriate fineness containing the crack [Figures 10 c) - e)]. The SIF is calculated with the J integral method. This is performed for various crack lengths with given increment Δa, while the direction of crack propagation is determined by the SIFs for Mode I and Mode II. The finite element model in FRANC2D does not contain contact elements. Therefore, the contact between the main and cover or lap plate was realized by additional elements in the gap having usual axial stiffness, but negligible shear stiffness.

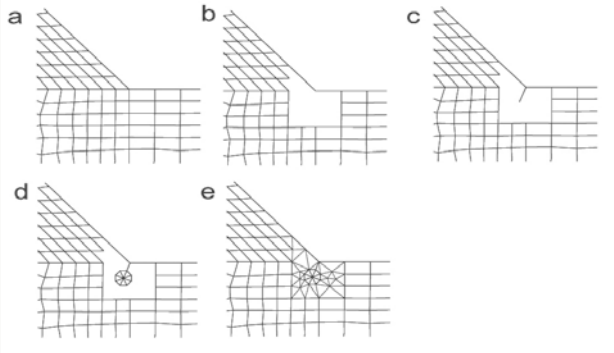

Figure 10 – Re-meshing around the crack tip in FRANC2D [17]

The fatigue life is determined using the computed SIFs and integrating Equation (3) numerically from the initial to the final crack length. The initial crack length a_i has been assumed as 0.1 mm, while the final crack length has been set to approximately half plate thickness. The remaining life is neglected.

Figure 11 shows typical crack paths computed for the weld toe and the weld root. While the crack at the weld toe follows approximately the direction along half the notch opening angle, the direction is almost vertical at the weld root which agrees with the observations in the tests at least in the middle part of the specimens.

4.3 Results and comparison with the tests

The fatigue life (number of load cycles N) has been determined with a nominal stress range $\Delta\sigma_n$ = 150 MPa in the main plate. From this, a characteristic fatigue strength based on nominal stress in the main plate was determined by extrapolating the result with a slope exponent $m = 3$ to $N = 2 \times 10^6$. Table 3 shows the results.

A comparison with Table 1 shows that the critical failure location is well predicted with the crack propagation approach. However, the characteristic fatigue strengths are rather low in comparison with those found in the tests (Figures 5 and 6) and given by the nominal stress approach.

A reason might be that the 2D analysis is rather conservative by assuming a continuous crack along the weld toe or root line, whereas the first part of crack propagation might be governed by semi-elliptical crack shapes showing a reduced crack propagation rate. Also crack closure effects might have contributed to this. Further investigations are considered to be necessary to avoid over-conservative results in simplified crack propagation analyses.

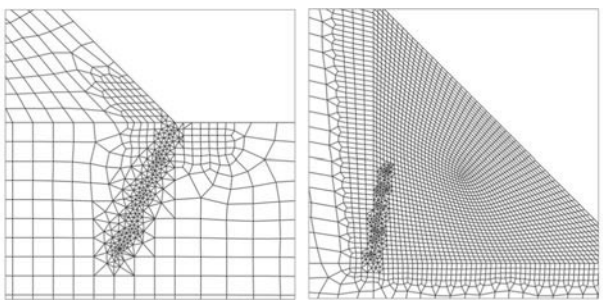

a) At the weld toe b) At the weld root

Figure 11 – Typical crack paths

Table 3 – Computed fatigue life N from crack propagation approach for $\Delta\sigma_n = 150$ MPa and derived characteristic fatigue strength $\Delta\sigma_c$

	Fatigue life N, crack at:		$\Delta\sigma_c$, crack at:	
	toe	root	toe	root
L.3	27 655	**12 352**	36.0	**27.5**
C.3	**70 917**	91 070	**49.3**	53.6
L.7	**85 641**	108 751	**52.5**	56.8
C.7	**117 248**	706 159	**58.3**	106.0

Critical failure location is indicated in bold.

5 Comparison of all results based on nominal stresses

Both applied approaches are able to compute the fatigue life of the four different specimen types for a given nominal stress range regarding weld toe and weld root failure. The characteristic fatigue strength at 2×10^6 cycles for a survival probability $P_s = 97.7$ % can be derived by extrapolating the results with a slope exponent $m = 3$ to this number of cycles.

A third approach being suitable for assessing weld toe as well weld root failure is the effective notch stress approach [2, 4] mentioned in the Introduction which uses a fictitious notch rounding at the weld toe and root, the latter normally by a keyhole shape. This approach has been applied to the specimen types in the previous study [11], where characteristic fatigue strengths have been derived as well.

Table 4 summarizes all computed characteristic fatigue strengths based on nominal stress in the main plate together with those derived from the measurement. The results for the thin welds (L.3 and C.3) show that the fatigue critical locations are quite well identified if the small difference between the values for the effective notch stress of C.3 is neglected. The same applies also to the cover plates with large weld throat thickness (C.7). However, the results of the crack propagation approach are generally too low compared with the test results as already discussed.

Only the fatigue-critical location for the lap joint with thick welds (L.7; toe failure) is partly not predicted. In the N-SIF approach this might be due to the too small control radius, whereas the result for the effective notch stress approach seems to be affected by the keyhole notch creating a too severe notch effect.

Table 4 – Characteristic fatigue strength $\Delta\sigma_c$ [MPa] based on nominal stresses in main plate and $m = 3$

Specimen type	L.3		C.3		L.7		C.7	
Crack location	toe	root	toe	root	toe	root	toe	root
Test	–	**47**	**73**	–	**73**	–	**73**	–
N-SIF approach[a)]	42.4	**34.3**	**60.9**	74.4	64.2	**57.6**	**73.5**	134.6
Crack prop. approach	36.0	**27.5**	**49.3**	53.6	**52.5**	56.8	**58.3**	106.0
Effective notch stress approach	39.1	**30.7**	63.5	**62.5**	67.2	**54.6**	**79.8**	100.4

a) with $R_0 = 0.28$ mm.
Fatigue-critical location is indicated in bold.

6 Conclusions

Only few approaches for the fatigue strength assessment of fillet-welded joints are able to consider both fatigue-critical locations, i.e. weld toe as well as weld root. In order to validate these approaches, fatigue tests were performed with 12 mm thick lap joints having full-load carrying fillet welds, and cover plates where the welds carry only part of the load in the plate. Two different weld throat thicknesses were realized (3 and 7 mm).

In the investigations described, two approaches have been applied to the specimen types mentioned: a newly-developed approach based on the notch stress intensity factor (N-SIF) and the well-known crack propagation approach. In addition, results of the effective notch stress approach have also been considered which were obtained in an earlier investigation.

From the tests and computations, the following conclusions are drawn:

1. Joints with large weld throat thickness show crack initiation at the weld toe, while a small weld throat thickness supports crack initiation from the weld root, particularly with full-load carrying fillet welds in lap joints.
2. Three test series with weld toe failure showed similar characteristic fatigue strengths. Here, the load carrying grade seems to have no effect on the fatigue strength. Only slight differences were observed between specimens in the as-welded and stress-relieved state.
3. The N-SIF approach can easily be applied when the relationship between the N-SIF and the averaged strain energy density in a control volume around the notch tip is utilized. The latter may serve directly as fatigue parameter.
4. The fatigue strength can be computed quite well with the N-SIF approach, however, the fatigue-critical location is only partly identified if the same control volume is used for the weld toe and root.
5. It has been found that the conversion of the averaged strain energy from a control radius of 1.0 mm to the smaller, recommended value of 0.28 mm, is possible but needs the evaluation of the T-stress component at the weld root, which plays an important role for the considered geometries. A conversion based only on the singular terms might result in large overestimations of the strain energy density.
6. The crack propagation approach identifies the fatigue-critical location very well. However, too small fatigue strengths were computed which might be due to the simplified 2D analysis neglecting semi-elliptical crack shapes. Also crack closure might have affected the results.
7. The identification of the fatigue-critical location seems to be more problematic with the effective notch stress approach. Here, the stress in the keyhole notch at the weld root can be over-estimated.

Further investigations are felt to be necessary to solve the shortcomings of the different approaches mentioned. Additional investigations might be necessary also to exactly quantify the 'out-of plane' mode coupled to the Mode II stress distributions at the weld toe, as recently documented by 3D numerical analyses carried out on welded lap joints.

Acknowledgements

The fatigue tests were performed within the Network of Excellence on Marine Structures MARSTRUCT (http://www.mar.ist.utl.pt/marstruct/), which was funded by the European Union through the Growth programme under contract TNE3-CT-2003-506141.

References

[1] Niemi E., Fricke W. and Maddox S.: Fatigue analysis of welded components – Designer's guide to the structural hot-spot stress approach, Woodhead Publishing, Cambridge, 2006.

[2] Hobbacher A.: Recommendations for fatigue design of welded joints and components, Doc. IIW-1823, WRC Bulletin 520, Welding Research Council, Inc., New York, 2009.

[3] Radaj D., Sonsino C.M. and Fricke W.: Recent developments in local concepts of fatigue assessment of welded joints, International Journal of Fatigue, 2009, vol. 31, no. 1, pp. 2-11.

[4] Radaj D., Sonsino C.M. and Fricke W.: Fatigue assessment of welded joints by local approaches, Woodhead Publishing (2nd Edition), Cambridge, 2006.

[5] Lazzarin T. and Tovo R.: A notch intensity factor approach to the stress analysis of welds, Fatigue & fracture of engineering materials & structures, 1998, vol. 21, no. 9, pp. 1089-1103.

[6] Livieri P. and Lazzarin P.: Fatigue strength of steel and aluminium welded joints based on generalised stress intensity factors and local strain energy values, International Journal of Fracture, 2005, vol. 133, no. 3, pp. 247–276.

[7] Lazzarin P., Berto F., Gomez F.J. and Zappalorto M.: Some advantages derived from the use of the strain energy density over a control volume in fatigue strength assessments of welded joints, International Journal of Fatigue, 2008, vol. 30, no. 8, pp. 1345-1357.

[8] Paris P.C. and Erdogan F.: A critical analysis of crack propagation laws, Trans. ASME, Journal of Basic Engineering, 1963, Series D, vol. 85, no. 4, pp. 528–534.

[9] Maddox S.J.: Assessing the significance of flaws in welds subject to fatigue, Welding Journal, 1974, Res. Suppl., vol. 53, no. 9, pp. 401s-409s.

[10] Petershagen H.: A comparison of two different approaches for the fatigue strength assessment of cruciform joints, IIW Doc. XIII-1410-91, 1991.

[11] Fricke W. and Feltz O.: Fatigue tests and numerical analyses of partial-load and full-load carrying fillet welds at cover plates and lap joints, Doc. IIW-2080, Welding in the World, 2010, vol. 54, no. 7/8, pp. R225-R233.

[12] Williams M.: Stress singularities resulting from various boundary conditions in angular corners of plates in extension, Journal of Applied Mechanics, (ASME), 1952, vol. 19, no. 4, pp. 526-528.

[13] Boukharouba T., Tamine T., Nui L., Chehimi C. and Pluvinage G.: The use of notch stress intensity factor as a fatigue crack initiation parameter, Engineering Fracture Mechanics, 1995, vol. 52, no. 3, pp. 503-512.

[14] Lazzarin P. and Zambardi R.: A finite-volume-energy-based approach to predict the static and fatigue behaviour of components with sharp V-shaped notches, International Journal of Fracture, 2001, vol. 112, no. 3, pp. 275-298.

[15] Williams M.: On the stress distribution at the base of a stationary crack, Journal of Applied Mechanics, 1957, vol. 24, no. 1, pp. 109-114.

[16] BS 7608: Code of practice for fatigue assessment of steel structures, British Standards Institution, London, 1993.

[17] Franc2D/L: http://www.cfg.cornell.edu/software/franc2d_casca.htm, 2004.

About the authors

Dipl.-Ing. Claas FISCHER (claas.fischer@tuhh.de), Dipl.-Ing. Olav FELTZ (feltz@tu-harburg.de) and Prof. Dr.-Ing. Wolfgang FRICKE (w.fricke@tu-harburg.de) are all with Institute of Ship Structural Design and Analysis, Hamburg University of Technology (TUHH), Hamburg (Germany). Prof. Paolo LAZZARIN (plazzarin@gest.unipd.it) is with Department of Management and Engineering, University of Padova, Vicenza (Italy).